Resistive and calorimetric investigations of an insulating quasicrystal *i*-AlPdRe

J. J. Préjean and J. C. Lasjaunias
Centre de Recherches sur les Très Basses Températures, CNRS, Boîte Postale 166, F-38042, Grenoble Cedex 9, France

C. Berger
Laboratoire d'Etudes des Propriétés Electroniques des Solides, CNRS, Boîte Postale 166, F-38042, Grenoble Cedex 9, France

A. Sulpice
Centre de Recherches sur les Très Basses Températures, CNRS, Boîte Postale 166, F-38042, Grenoble Cedex 9, France
(Received 2 June 1999; revised manuscript received 15 November 1999)

We report on resistivity, magnetic susceptibility, and very low-T specific heat (C_p) of a *i*-AlPdRe quasicrytalline sample which, from resistivity measurements, is believed to lie on the insulating side of a metal-insulator (MI) transition. We find an electronic contribution to C_p, which possibly obeys a γT variation above 1 K but follows a power T^a law ($a \sim 0.1$–0.3) below 1 K, in agreement with early results obtained for systems crossing the MI transition. We point out the dependence of the lattice term on the method of sample preparation. Finally, from a comparative study of *i*-AlCuFe and *i*-AlPdMn systems, we show that the large nuclear hyperfine specific heat in AlPdRe, dominant below 300 mK, is of quadrupolar origin, due only to the Re nuclei.

I. INTRODUCTION

The icosahedral phase *i*-AlPdRe presents the most striking electronic properties among the high structural quality quasicrystalline phases. In *i*-AlPdRe samples, the reported resistivity can reach values as high as for semiconductor based systems on the insulating side of the metal-insulator transition,[1,2] with similar temperature dependences.[3] Attempts to understand this intriguing resistive behavior in an alloy consisting only of metallic elements have taken into account the specific structural aspects of icosahedral phases. These include the role of quasiperiodicity, of specific icosahedral packing of atoms,[4,5] but also the role of possible residual disorder and electron-electron interactions.[6] Indeed, no experiment so far indicates the opening of a gap as in semiconductors. A reduced electronic density of states was, however, reported in *i*-AlPdRe by specific-heat measurements (about one-tenth of that of pure aluminum),[1,7,8] and by electron spectroscopy.[9,10] There are also indications for a rapidly varying electronic density of states around the Fermi level, by tunneling spectroscopy,[11–13] and nuclear magnetic resonance.[14,15]

However, it was noticed that the transport properties of the *i*-AlPdRe phase crucially depend on the conditions for sample preparation. For instance, the low-temperature dependence of resistivity $\rho(T)$ can strongly vary between samples prepared by different processes.[2,16] Even in the same batch of samples, the ratio ρ_{4K}/ρ_{300K} can be varied by a factor more than 2 for different samples.[2] From conductivity and magnetoconductivity measurements, we believe that the lower conducting *i*-AlPdRe samples (ratio $\rho_{4K}/\rho_{300K} \geqslant 20$–$30$ typically) may be on the insulating side of the metal-insulator transition, whereas the higher conducting one (ratio $\rho_{4K}/\rho_{300K} \leqslant 10$–$15$) would still be in the metallic region.[2,3] It is thus of prime importance to measure all related properties on the same sample. We previously analyzed[2,17] the transport properties of a series of *i*-AlPdRe samples that approach and possibly cross the metal-insulator transition.[2,3] The highly resistive *i*-AlPdRe samples provide a unique opportunity for studying the physical properties of a quasicrystal believed to be on the insulating side of the metal-insulator transition. It is the aim of the present paper where we present specific heat, resistivity, and magnetic susceptibility measurements on a sample characterized by a high resistivity ratio: ratio $\rho_{4K}/\rho_{300K} = 80$.

Three main conclusions can be derived from our analysis of the specific-heat data. The first one is that we could not show evidence for the existence of a sizeable linear term in the specific heat $C_p(T)$ below 1 K. A γT term could be extracted from the C_p data only above 1 K: $\gamma \approx 0.1$ mJ/mol K^2, which is in agreement with other studies,[1,7] although samples were there produced by different techniques and seemingly possess different transport properties. In contrast, below 1 K down to 100 mK, we can well account for our data by introducing a nonlinear term T^a ($a = 0.1$–0.3) which we can attribute to the onset of localization and/or two-level systems. The second conclusion, yielded by the latter analysis, is that the electronic density of states $N(E)$ at the Fermi level E_F is very small compared to normal metals, with a maximum value $N(E_F) \approx 4 \times 10^{-2}$ state/eV atom, corresponding to a maximum estimate of the γ value deduced above 1 K. This is confirmed by the diamagnetic susceptibility of our *i*-AlPdRe sample. The third conclusion concerns the hyperfine term of $C_p(T)$, which we can attribute unambiguously to the Re nuclei, thanks to a comparison with specific-heat data obtained previously on other close related systems (*i*-AlCuFe, *i*-AlPdMn).

II. SAMPLE PREPARATION AND CHARACTERIZATION

Pure Al ($5N$), Pd ($4N$), and Re ($4N$) elements were melted together under purified argon atmosphere by arc

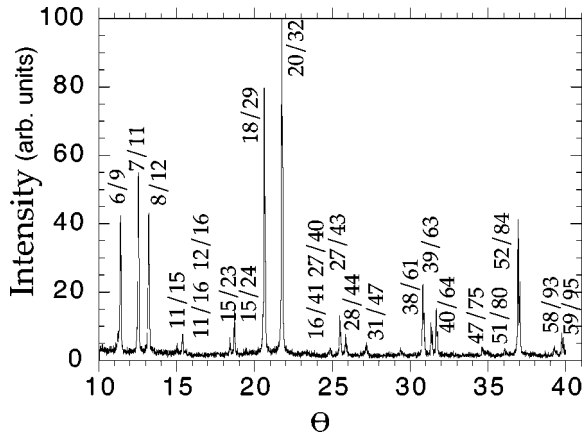

FIG. 1. X-ray-diffraction pattern of the *i*-AlPdRe sintered pellets used in the specific-heat measurements (Cu $K\alpha$ radiation). All the peaks are indexed with the *i* phase.

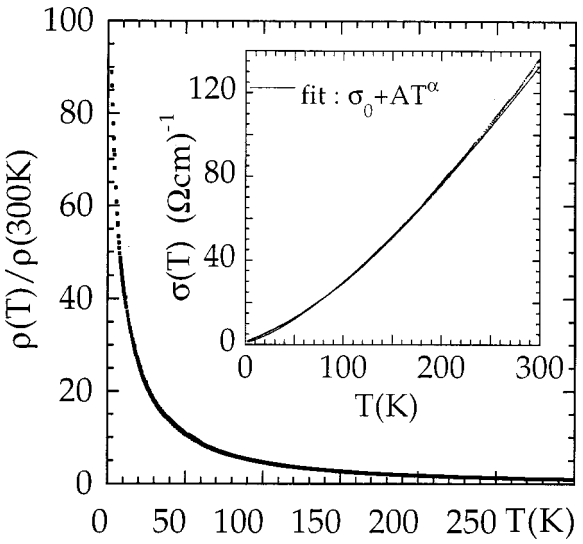

FIG. 2. Temperature dependence of the resistivity of our *i*-AlPdRe sample.

melting and by subsequent induction in an electromagnetic levitation cold crucible. The ingots of nominal composition $Al_{70.5}Pd_{21}Re_{8.5}$ were then melt spun into ribbons. Sintered pellets were prepared from crushed ribbons and annealed at high temperature (up to 1000 °C). Great care was taken to optimize the preparation process in order to get homogeneous and highly resistive samples.[2] We have chosen to measure a sintered pellet (115 mg mass) in order to obtain a single piece of material large enough to be reliably measured in our specific-heat apparatus. This also allows resistivity measurements, which is a crucial information to check the actual quality of the measured sample.

Figure 1 presents the x-ray-diffraction pattern of the sintered pellets we measured. All the peaks can be indexed with the single icosahedral phase (no extra peaks, no shoulder in the peak profiles). Note that no other phases are detected, to the resolution of standard x-ray diffraction, that we were able to detect in other types of samples.[18]

No structural model is so far available for the icosahedral phase of AlPdRe. However, it is reasonable to assume that the structure is similar to that of *i*-AlPdMn, considering an isomorphous substitution of Mn by the isoelectronic Re. Indeed, all the peak positions of the x-ray-diffraction pattern of Fig. 1 can be exactly deduced from those of the *i*-AlPdMn, provided the six-dimensional unit-cell parameter a_6 is inflated in *i*-AlPdRe compared to AlPdMn ($a_6=6.53$ and 6.452 Å, respectively). The latter value was determined for AlPdMn in a high-resolution powder experiment.[19] Also it was shown that the partial substitution of Mn by Re leads to an icosahedral phase as well.[20]

III. ELECTRICAL CONDUCTIVITY

Resistivity was measured from 2 to 300 K by the standard four-probe method in a continuous flux cryostat. The absolute value of the electrical resistivity was determined from weighting the sample, thus taking into account the exact amount of material in the sample, which is generally overestimated by simple geometrical measurements. We already pointed out[2,17] a relation between the temperature dependence of the resistivity ρ, summarized in the ratio ρ_{4K}/ρ_{300K}, and its absolute value. Hence our samples can be characterized by their resistivity ratio.

The resistivity measurement is only taken in this paper as a characterization for the sample quality. The transport behavior of the *i*-AlPdRe phase is described in greater detail elsewhere.[2,3] Figure 2 presents the temperature dependence of the resistivity for the sintered pellet. The absolute value was estimated to be $\rho_{4K}\approx 0.5\ \Omega$ cm, and the temperature dependence yields to $\rho_{4K}/\rho_{300K}=80$. Such high resistivity and ρ_{4K}/ρ_{300K} ratio are indications for the high structural quality of the sample. Indeed, defects of stochiometric composition or tiny fraction of secondary phase (not detected by x-ray diffraction) are expected to give a more metallic behavior.

We note in Fig. 2 that the conductivity $\sigma(T)$ of our *i*-AlPdRe sample obeys to the first order a simple power law $\sigma(T)=\sigma_0+AT^x$ with $x\approx 1.4$ in the range 50–300 K. This value of x for a sample of resistivity ratio $\rho_{4K}/\rho_{300K}=80$ follows our previously noticed correlation[2] in a series of *i*-AlPdRe ribbons for which the lower the conductivity, the higher ρ_{4K}/ρ_{300K} and the higher the exponent x. The x values range between 1 and 1.5 for ρ_{4K}/ρ_{300K} ranging from 2 to 100, respectively. Contrary to reported data for the intermetallic Al_2Ru, believed to be a semiconductor and exhibiting a real gap in the electronic density of states,[21] the conductivity of *i*-AlPdRe does not follow the temperature activated law $\sigma(T)\sim\exp(-\Delta/T)$ in any temperature range between 2 and 300 K. For ribbon samples of similar ρ_{4K}/ρ_{300K} value ($\rho_{4K}/\rho_{300K}=84$), we recently showed[3] that $\sigma(T)$ at much lower temperatures (below 600 mK) drops similarly to disordered insulator systems with a Mott's-type law for variable range hopping. The overall conductivity features [σ_0 value, $\sigma(T)$ dependence in the whole 20 mK–300 K range] are quite similar to those of insulating In-O close to the metal-insulator transition. Therefore it sounds reasonable that the present pellet also lies in the insulating region. Indeed, it is made of identically produced ribbons and has the same electrical characteristics (ρ_{4K}, ρ_{4K}/ρ_{300K}, x).

IV. MAGNETIC MEASUREMENTS

Using a superconducting quantum interference device magnetometer (Metronique) of sensitivity 10^{-8} emu, we

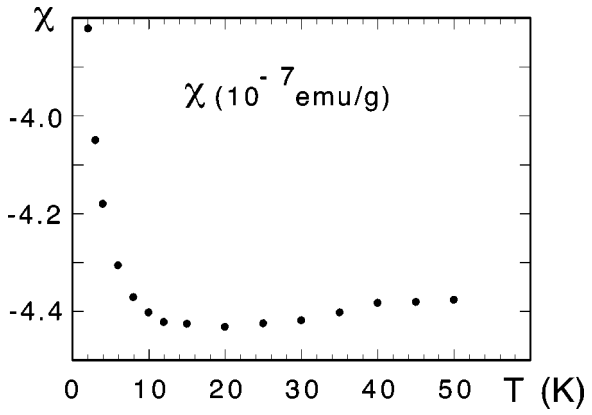

FIG. 3. Temperature dependence of the susceptibility.

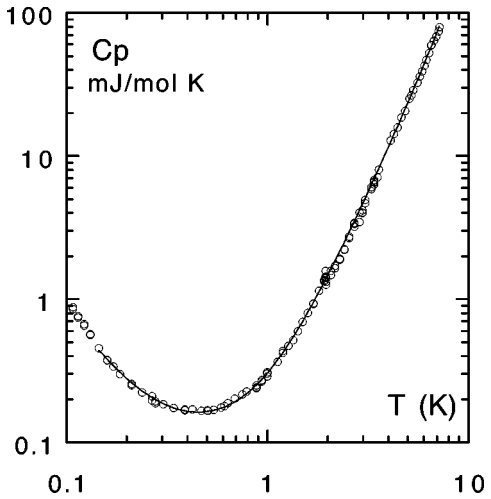

FIG. 4. Temperature dependence of the specific heat C_p vs T in a log-log diagram. Data below 250 mK are obtained from an approximate analysis of the thermal response decay described in Sec. V A.

measured the susceptibility χ of our sample in the range 2–50 K in a field $H=0.1$ T. In Fig. 3 we present our data in a χ vs T diagram. The data can be fitted with a law including a paramagnetic term C/T superimposed to a diamagnetic term χ_0:

$$\chi=\chi_0+C/T.$$

We obtain a large negative value of χ_0: -4.6×10^{-7} emu/g. This implies that the positive Pauli susceptibility χ_P, which adds to the diamagnetism, is very small. As χ_P is due to the conduction electrons at the Fermi level E_F, we conclude that the electronic density of states at E_F is very small. We found a quite small Curie constant: $C=1.5\times10^{-7}$ emu/g, which is however 23 times larger than that calculated for the nuclear magnetism, taking into account the values of the nuclear magnetic moments of the different elements: Al, Pd, Re. Thus the origin of the Curie term C/T is to be found in the presence of paramagnetic impurities. As we will show in the following, we have to make sure that the magnetic atoms are of small quantity in order to draw reliable conclusions from the specific-heat data. We know that impurities exist already in the initial constituents. For instance, the chemical analysis of Al, Pd, and Re given by the supplier allows us to estimate a concentration of about 9 ppm of Fe atoms in our sample. Also, some contamination can occur in the preparation of the sample. It remains that the small magnitude of Curie constant implies the presence of only a very few magnetic atoms. For instance, by assuming a concentration of magnetic moments μ of about 10 ppm, we find a reasonable value for μ: $3\mu_B$. This allows us to rule out the possibility of contributions of magnetic origin to the specific heat.

V. SPECIFIC HEAT—EXPERIMENTAL RESULTS

A. Experimentals, problems due to time effects

Specific-heat measurements were performed with the same transient heat-pulse technique[22] on a dilution refrigerator between 0.1 and 7.2 K, as previously for other quasicrystelline samples.[23] The data are shown in a log-log plot of $C_p(T)$ vs T in Fig. 4. As we will show in the next section, the rapid increase of $C_p(T)$ with the temperature T above 1 K can be attributed to the contribution of the lattice, whereas, below 300 mK, the large increase of $C_p(T)$ at decreasing temperatures is due to a large nuclear hyperfine term varying as T^{-2}.

However, due to the small mass of the sample, the relative contribution of addenda to C_p, measured in separate experiments, appears to be important above 1 K. It is about 65% of the total heat capacity between 1 and 7 K, which explains the scattering of data as seen in Fig. 4. At lower T, the increasing contribution of a nuclear hyperfine term in the sample reduces the relative addenda contribution to less than 10% below 0.2 K.

As we will show in the following, we encountered serious problems to extract accurate values of the specific heat at the lowest temperatures, due to nonconventional thermal response of the sample. This requires to outline a specific property of our sample arrangement. Several nylon pins are used to press the sample between two silicon plates (one equiped with the heater, and the opposite one with the thermometer). The thermal resistivity $\rho_{th}(T)$ of the nylon pins which are linked to the cold source (temperature T_0) determines essentially the thermal resistance R_l between the sample and the cold source: $R_l=G\rho_{th}(T)$. The geometric factor G depends on the length of the pins and the pressure at the contact surface which can vary quite largely between different experiments, following the thickness and stiffness of the sample. But the thermal dependence of $\rho_{th}(T)$ remains unchanged. This has been verified over several tens of experiments using the same experimental equipment. With our method, once the heat pulse (energy E, duration 0.1–0.2 s) has been applied at time $t=0$, the temperature, initially at value T_0, increases rapidly. The characteristic time of the T rise is governed by the diffusivity of the sample and the coupling to the phonon bath of all the ingredients (lattice, electrons, nuclei, ...) which rapidly absorb the energy. Subsequently the temperature decreases down to the equilibrium temperature T_0. Then, in the simplest case, the T decay obeys an exponential law: $T=T_0+\Delta T\exp(-t/\tau)$. The total heat capacity $C_{p.tot}$ of the sample + addenda is given by $C_{p.tot}=E/\Delta T$, and the relaxation time by $\tau=R_lC_{p.tot}$. This

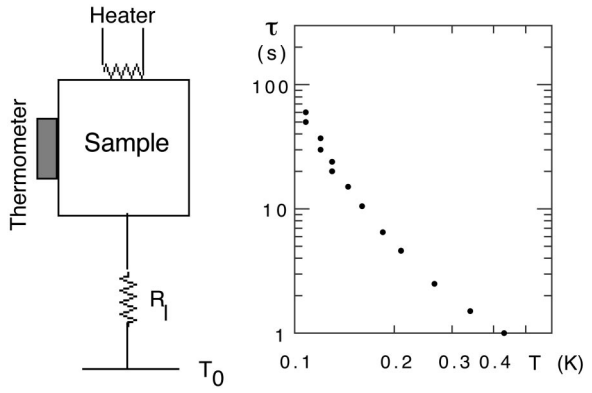

FIG. 5. Left side: schematic diagram of the experiment. Right side: temperature dependence of the characteristic time of the thermal response to a heat pulse involved in our C_p measurement.

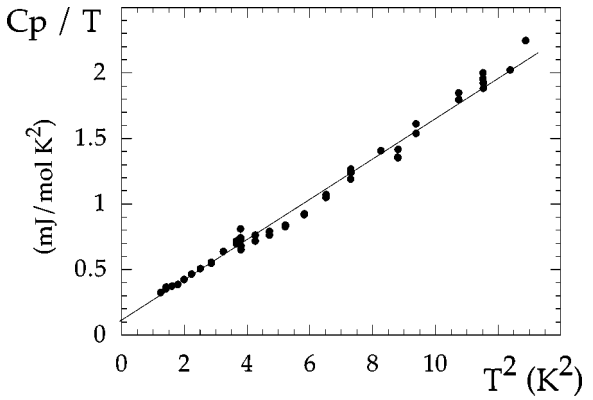

FIG. 6. Temperature dependence of specific heat C_p/T vs T^2 between 1 and 3.6 K. The fit of the data between 1 and 3.6 K corresponds to $C_p=\gamma T+\beta T^3$, with $\gamma=0.11$ mJ/mol K^2 and $\beta=0.15$ mJ/mol K^4.

behavior is well observed in the present experiment above 300 mK, and we check the self-consistency of our analysis by verifying that $\tau/C_{p.tot}$ follows accurately the temperature dependence of $\rho_{th}(T)$ observed in previous experiments. For information, in the present experiment, the time constant τ decreases from 13 s at 7 K to 0.7 s at 0.7 K (minimum of time constant). At decreasing temperatures below 0.5 K, the occurence of a large contribution of the nuclear term has in consequence a rapid increase of $\tau=R_lC_{p.tot}$ (see Fig. 5) since not only $C_{p.tot}$, but also R_l increases rapidly (as $T^{-2.3}$ below 300 mK) at decreasing temperatures.

Below 250 mK, an additionnal problem arises for the present experiment: the recovery of the equilibrium temperature deviates from an exact exponential behavior at both short and long times. These deviations are more and more pronounced when the temperature is decreased. So the experimental determination of C_p depends on the time span. This question of anomalous thermal dynamics and the consequences on the value of C_p will be discussed in detail in a forthcoming paper.[24] In order to minimize this problem, we have to use the following method to analyze our data: first we estimate the value of $R_l(T)$ in this range of temperature. Indeed, since we know the temperature dependence of $R_l(T)$ in all the temperature range (see above), we could extrapolate with confidence the R_l value below 250 mK, from R_l values well defined in the higher T range. Second, we imposed to fit the temperature relaxation by a single exponential of time constant τ, in a time window chosen to recover the order of magnitude of $R_l(T)$ from $\tau/C_{p.tot}$. These values of τ are reported in Fig. 5. We have used a time span after the heat pulse of the same order as the relaxation time τ itself, i.e., from about 15 s at 150 mK to 60 s at 110 mK.

B. Possible contributions to C_p

In order to analyze our data presented in Fig. 4, we have to take into account all the different contributions which can be expected for this system. First, we attribute the large upturn of $C_p(T)$ at low temperatures to the contribution of a nuclear hyperfine term which yields a T^{-2} term. It can originate in effective hyperfine magnetic fields or in electrical-field gradients. Second, we have to consider both the lattice contribution $C_{lat}(T)$ and a linear T term ($\gamma_{el}T$) due to the conduction electrons, with γ_{el} proportional to the electronic density of states $N(E_F)$ at the Fermi level E_F. Third, other low-T excitations can contribute noticeably to $C_p(T)$, for instance, those due to electronic localization or to the low-energy configurational excitations such as two-level tunneling states (TLS). Both these contributions generate terms which can follow power laws of T in a given temperature range, with a value of the exponent which can be different from 1. The presence of a nonlinear term was already evidenced by the low-temperature specific heat of *i*-AlCuFe.[23] Let us first discuss the possible TLS contribution to the specific heat. In the present case, a TLS contribution can exist since TLS excitations have been detected in perfect quasicrystals, either by acoustic measurements in *i*-AlPdMn[25] or by thermal conductivity measurements in *i*-AlPdMn[26] and *i*-AlPdRe[7] or from NMR.[27] We recall that TLS excitations give rise to Shottky anomalies in the specific heat. It results in a T^ν term at low temperatures in the case where there exists a broad distribution $P(\Delta)$ of the splitting energies. The value of the exponent ν depends on the exact distribution $P(\Delta)$. It is easy to calculate the exponent ν at temperatures much smaller than the width of $P(\Delta)$: for a flat distribution $P(\Delta)$, we have $\nu=1$ (i.e., $C_{TLS}=\gamma_{TLS}$ T), while for $P(\Delta)\sim(\Delta)^{-u}$, with $0<u<1$, we have $\nu=1-u<1$. For instance, a value of $\nu=0.5$ has been reported in amorphous metallic alloys.[28]

Now a contribution specific to the electronic localization could also occur. Indeed, there are indications for localization of electrons in electrical transport measurements in *i*-AlPdRe phases of high resistivity.[1,3] And for systems other than QC's, known to be close to a metal-insulator transition, the specific heat has been observed to deviate broadly from a linear T behavior at low temperatures. For instance, it is the case of Si:P below 1–2 K where the electronic specific heat reveals to depend very little on the temperature down to 0.2 K. In that case, C_p can be expressed[29] in terms of a power law of T: $C_p(T)\sim C_{el}T^\mu$, $\mu<1$. In consequence, we can expect that the specific heat for our sample obeys in the more general way the law

$$C_p=C_NT^{-2}+\gamma_{TLS}T^\nu+C_{el}T^\mu+C_{lat}(T), \qquad (1)$$

where the standard term $\gamma_{el}T$ is recovered for $\mu=1$ (then $C_{el}=\gamma_{el}$). Now we present two types of analysis. The first

TABLE I. Results of different specific-heat analyses performed in different temperature intervals, as described in the text.

		Electronic + TLS term			Hyperfine term	Lattice terms	
Analysis	T range (K)	γ (mJ/mol K^2)	A (mJ/mol K^{1+a})	a	C_N (μJ K/mol)	β (mJ/mol K^4)	δ (mJ/mol K^6)
$\gamma T+\beta T^3$	1–3.6	0.11				0.15	
$\gamma T+\beta T^3+\delta T^5$	1–7.2	0.11 (fixed)				0.15	1.3×10^{-3}
$\gamma T+C_N T^{-2}$	0.107–0.2	?			9.7 ± 0.3		
$C_N T^2+AT^a+\beta T^3$	0.14–1.6		0.14	0.25 ± 0.05	7.5	0.16	
	0.3–1.6		0.13	0.1 ± 0.05	6.5	0.16	
$C_N T^{-2}+AT^a+\beta T^3+\delta T^5$	0.14–7.2		0.14	0.25	7.5	0.16	1.1×10^{-3}

one is the standard one, used for most metallic alloys:

$$C_p = C_N T^{-2} + \gamma T + C_{lat}(T) \quad (2)$$

with the usual Debye law for the lattice contribution. The second type of analysis takes into account the possibility of contributions giving T^ν, T^μ terms (with $\nu,\mu<1$) and of additionnal nonusual modes in the lattice vibrations.

C. Standard analysis

The standard analysis allows us to compare our results with those of previous authors who used expression (2) to fit their data. Then, the TLS contribution can be involved but with the simplest case of $\nu=1$:

$$\gamma = \gamma_{el} + \gamma_{TLS}.$$

Also we use the usual expression $C_{lat}(T)=\beta T^3+\delta T^5$ for the lattice contribution. We found that expression (2) could account for our results only above 1 K and below 0.3 K. Above 1 K, where we neglected the T^{-2} term, a single T^3 term appears to be sufficient up to 3.6 K to analyze the lattice contribution. This is shown in Fig. 6 where the data, plotted in a C_p/T vs T^2 diagram, are aligned on a straight line. We found a large value of $\beta=0.15$ mJ/mol K^4. Consequently, it is difficult to extract a precise value of γ which reveals to be very small. Thus we can give only an approximate value of γ: 0.11 ± 0.05 mJ/mol K^2. To account for the data at higher temperatures, we have to add a usual T^5 term:

$$C_p(T) = \gamma T + \beta T^3 + \delta s T^5. \quad (3)$$

In order to analyze our data up to 7.2 K where the lattice contribution is overdominant, we fixed the γ value to 0.11 mJ/mol K^2 as deduced previously. Then we recovered the previous value of β and found $\delta=1.3\times10^{-3}$ mJ/mol K^6.

At the lowest temperatures, say below 300 mK, the lattice contribution becomes totally negligible. For instance, at 300 mK, taking for β the value deduced above, we predict that C_{lat} equals 3% of the measured specific heat. Thus we expect to be able to fit our data by the restricted law

$$C_p = \gamma T + C_N T^{-2}$$

which should provide the values of both γ and C_N. Actually, it is difficult to deduce reliable values of these two parameters in the range of temperature 0.1–0.3 K, for the following reasons. First, the predicted value of γT (by using the value of 0.11 for γ determined above 1 K) is much smaller than the nuclear term at the lowest temperatures. For instance, at 100 mK, we calculate a value of γT as low as 1.1% of the total specific heat. Second, the precision of our C_p data below 250 mK is lowered due to the time constant effects as explained in Sec. V A and in Ref. 24. At this stage, we could only note that C_pT^2 is rather constant below 170 mK: $C_pT^2\approx9.7\pm0.3\times10^{-3}$ mJ K/mol. This value gives a first estimation of C_N. Now, in the 0.3–1.6-K range of temperature, we can expect to extract a more reliable value of γ. Indeed, in this temperature range, no complication due to the thermal dynamics occurs and the hyperfine as well as the lattice terms are not too large. In a first attempt, we calculated the amplitude of the specific heat from Eq. (2) with the values of C_N, γ, and β deduced above (see Table I): it is represented by a dashed curve in Fig. 7. It appears to differ widely from the experimental data in the 0.5-K region. No other set of the parameters could provide a fit of the data of better quality in the 0.3–1.6-K temperature range.

D. Alternative analysis

While an accurate fit of the data could not be done in the previous analysis below 1 K , we could nicely fit C_p once we replaced the γT term by a power law of T with an exponent different from 1:

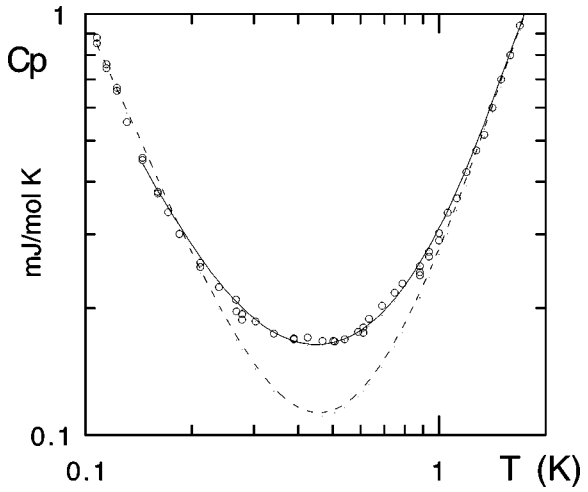

FIG. 7. Specific heat in the range 0.1–1.6 K. Open circles: experimental data; dashed curve: calculated value including a linear T term [formula (2)] and matched to the value of C_p at 108 mK; solid curve: fit including a T^a term [formula (4)].

$$C_p(T) = C_N T^{-2} + A T^a + C_{lat}(T). \quad (4)$$

This expression allowed us to fit very accurately our data in the range 140 mK–1.6 K (see Fig. 7), with the simplest assumption for the temperature dependence of the lattice contribution: $C_{lat}(T) = \beta T^3$. We found a value of the exponent $a \approx 0.25 \pm 0.05$, i.e., much smaller than 1. The value of C_N: 7.5×10^{-3} mJ K/mol, is found to be smaller than our previous estimate by 20%. However, we find a value of β for the lattice contribution close to that deduced in the standard analysis. It is also the case for the parameter δ used to fit the data up to 7.2 K. The values of the parameters, reported in Table I, allow us to fit the data over the 140-mK–7.2-K temperature range (see solid curve in Fig. 4).

Here we note that the same analysis restricted to data for which no anomalous dynamics are observed (i.e., above 300 mK) provides even smaller values of a and C_N: $a \approx 0.1, C_N \approx 6.5 \times 10^{-3}$ mJ K/mol (see Table I). Finally, we note that a different expression for C_{lat} like $B\,T^{3+b}$, as it was discussed in Ref. 23 for *i*-AlCuFe, allows a fit of equal quality to our data over the whole range of temperatures (140 mK–7.2 K) with $b = 0.4$ and a value for the exponent $a \approx 0.5$–0.7 slightly different from the previous one.

VI. DISCUSSION OF THE FOUR MAIN CONTRIBUTIONS TO THE SPECIFIC HEAT

A. Linear T term above 1 K

First, we discuss the amplitude of the linear T term which we could extract only above 1 K, using the standard analysis of C_p. It yields a very small value of $\gamma\,(=\gamma_{el}+\gamma_{TLS})$: $\gamma \approx 0.11$ mJ/mol K^2, which is about one order of magnitude smaller than that expected for the contribution of free electrons. It means a very small electronic density of states $N(E_F)$ at the Fermi level, when it is compared to normal metals: $N(E_F) \sim 3\gamma_{el}(\pi k_B)^{-2} \leqslant 4 \times 10^{-2}$ state/eV atom. This value of γ comparates well to those found above 1 K by other groups.[1,7] But in contrast with our case, Chernikov *et al.*[7] could account accurately for their data with this linear T term down to 70 mK for a sample of nominal composition slightly different from the one studied here. We will discuss this point in Sec. VI B. We outline that our value of γ is of the order of magnitude expected for TLS contributions in amorphous materials, such as oxide insulators or metallic alloys.[30] It is therefore possible that only a part of γ is actually due to the electronic contribution as already pointed out in Ref. 7. This would imply an even lower electronic density of states at E_F. Nevertheless, if we assume that γ is only due to the conduction electrons, we note that the conductivity is not simply proportional to the electronic density of states at the Fermi level, i.e., to γ. Indeed, in the present case, we found a value of γ not so different from that: $\gamma \sim 0.3$ mJ/mol K^2 of *i*-AlCuFe (from different groups: see Ref. 23 and references quoted therein), although the resistivity at 4 K of *i*-AlCuFe is about two orders of magnitude smaller than that of the present *i*-AlPdRe. The nonproportionality between γ and the conductivity for two different QC states of *i*-AlPdRe has been also pointed out by Pierce, Guo, and Poon.[1] Actually, the conductivity depends not only on $N(E_F)$ but on the electronic diffusivity which could play a major role to explain the very low conductivity in quasicrystals (see Ref. 31 and references quoted therein). And even the empirical relation $\sigma(4\,\mathrm{K}) \sim N^2(E_F)$, found for a large series of quasicrystals[32,33] and argued to follow Mott's theory for systems with E_F in the pseudogap, seems not to apply to the AlPdRe case.

B. T^a ($a<1$) contribution and metal-insulator transition

In our alternative analysis, we found that the addition of a contribution of the form AT^a is necessary to account for the data below 1.6 K. The small value of the exponent a implies that this contribution varies very little with T in the range 300 mK–1.6 K . We note that it was not necessary to maintain an additional linear T term to fit our data accurately. Two scenarios are then possible. First, the T^a term originates in TLS excitations. Then, we deduce that the electronic density of states at the Fermi level is too small to give a sizeable γT term. Second, the T^a term is due to the localization of electrons. Then, the electronic density of states at the Fermi level is not necessarily so small, but the electronic specific heat can present an unusual behavior. It is the case of doped semiconductors, for instance, for Si:P,[29] when the density of carriers is smaller than a critical value. In that case, the specific heat is found to be rather flat in the T range 200 mK–1.5 K, while the γT term defined by the density of states at E_F is recovered above 1.5 K. This behavior is quite similar to that which we deduced for our sample in the same range of temperature: in the 100-mK–1-K temperature range where the electronic specific heat is almost constant and also above 1 K where the standard analysis of C_p applies well, which means the possible recovery of a linear T term. The similarity between the specific heat of our sample and that of Si:P may not be fortuitous. Indeed, we believe that our sample, of resistivity ratio $\rho_{4K}/\rho_{300K} \approx 80$, is on the insulating side of the metal-insulator (MI) transition. In contrast, we expect a standard linear T term in the specific heat down to the lowest temperatures for systems lying on the metallic side of the MI transition. This should be the case for ''metallic'' *i*-AlPdRe samples, i.e., of smaller ratio[2,17] $\rho_{4K}/\rho_{300K} < 10$–$15$. Such a γT term has been observed previously[7] down to 65 mK for a AlPdRe sample[34,35] of $\rho_{4K}/\rho_{300K} < 10$, which is consistent with our interpretation.

C. Lattice contribution

We could account for the lattice contribution with a standard law, $C_{lat}(T) = \beta T^3 + \delta T^5$, in our two previous types of analyses: standard and alternative. We deduced nearly the same values for β and δ in both analyses (see Table I). The value of β implies a Debye temperature $\theta_D = (12\pi^4 N k_B/5\beta)^{1/3}$ of 235 K which is surprisingly small compared to several previous results [380 K (Ref. 7) and 450 K (Ref. 1)]. Indeed, the present β term is anomalously high: from four to seven times larger than that reported by other groups. Also we deduced a δ value seven times larger than that found by Pierce, Guo, and Poon.[1]

We recall that our sample is a sintered pellet prepared from crushed ribbons and not an ingot. Previously, we have observed a similar enhancement of C_{lat} for ribbons of *i*-AlPdMn and *i*-AlCuFe obtained by melt spinning, in com-

parison to what we measured for single QC grain (*i*-AlPdMn) or for several polyquasicrystalline ingots (*i*-AlCuFe).[36] It is worth noting that the specific heat of ribbons of various phases (stable QC's: AlCuFe, AlPdMn, the present AlPdRe, as well as metastable AlMn) is very similar above 4 K where C_{lat} dominates. Then, it is found that a typical value of 100 mJ/mol K at T=5–6 K. This value is independent on the C_p behavior at low temperatures which depends broadly on the compound. At 5–6 K, the value of $C_p(T)$ for ribbons exceeds that of ingots of the same composition by a factor of 4 in the case of AlPdMn and even by a factor of 10 for *i*-AlCuFe system.[37] One could imagine the large magnitude of C_{lat} for ribbons to be due to a less high structural quality, compared to that of ingots, although no differences can be detected from x-ray-diffraction patterns. But it seems not to be the case when one considers the often accepted resistivity criterion: the larger the electrical resistivity, the better the structural quality. Indeed, different $C_{lat}(T)$ contributions are reported for *i*-AlPdRe samples (one ingot[1] and the present sintered pellet) having similar temperature dependence of resistivity. And in the case of *i*-AlCuFe, the $C_{lat}(T)$ term is much higher in a ribbon sample ($\rho_{4K} \approx 10\,000\ \mu\Omega$ cm for $AlCuFe_{12.5}$) than for an ingot having a much lower resitivity [$\rho_{4K} \approx 4400\ \mu\Omega$ cm for $AlCuFe_{12}$ (Ref. 23)]. Also, the presence of magnetism does not explain the enhancement of C_{lat}. Indeed, we found a much larger C_{lat} for ribbons of *i*-$AlPdMn_{7.5}$ (Ref. 36) than for an ingot containing 9.6 at. % Mn, which is 40 times more magnetic.[38]

Now, considering the thickness of ribbons of about 30 μm, we cannot attribute the unexpected large vibrational contribution to standard surface modes as could be expected in nanoparticules since the ratio of the number of atoms strictly at the surface to that in the volume is small. The same conclusion applies for the possible surfacelike modes of the small quasicrystalline grains (typical linear size: a few μm) which compose the ribbons. Then the number of atoms at the border of a grain is about 10^{-4} times that in the volume. A possible explanation for the large value of β could be found in an anomalous phasonlike contribution to C_p. Its origin could be in the atoms located in the grain boundaries although the latter have been observed to be thin. Already, it has been stressed that a quasicrystalline single grain of AlCuFe with the presence of volume phason-strain fields exhibits a value of β which is 2.5 times larger than that of an identical phason-free sample.[39] In our case, due to the grain boundaries, there exists a fraction of the total volume of a ribbon, which is of the order of a few 10^{-4}, which does not obey the strict quasiperiodic structure of the bulk. Thus this volume fraction, even small, could give a large additional contribution to vibrational specific heat. More studies are necessary to give a definite explanation to this anomalous specific-heat behavior.

D. Quadrupolar origin of the nuclear hyperfine contribution

We now turn to the nuclear hyperfine contribution C_N/T^2. We have found a C_N value: (9.7 ± 0.3) μJ K/mol and 7.5 μJ K/mol of alloy from the first and second analysis, respectively, in good agreement with the value $(8.23\pm0.04$ μJ K/mol) obtained by Chernikov *et al.*[7] in *i*-$Al_{70}Pd_{21.4}Re_{8.6}$. We note that we found a smaller value of C_N (6.5 μJ K/mol) when we restricted our second analysis to the temperature range where no anomalous dynamics are observed (i.e., above 300 mK). This is well understood, taking into account the thermal dynamical effects at the lowest temperatures (see Sec. V A and Ref. 24), which reveal a delayed response of a part of Re nuclei. Now, we demonstrate that the C_N/T^2 term is of quadrupolar origin, due to the Re nuclei. Concerning the origin of C_N, only two possible sources of nuclear specific heat exist: namely, magnetic and quadrupolar origins. We now discard the former which is due to the presence of magnetic atoms. In this case, C_N comes from the interaction, at the nucleus site, between the nuclear spin and the effective magnetic field induced by the electronic magnetization of the atom. For instance, such magnetic hyperfine interaction arises for magnetic Mn atoms in crystals as Cu-Mn as well as in quasicrystals Al-Mn and AlPdMn.[38] It was found in previous $C_p(T)$ and susceptibility studies[40] a ratio of C_N to the concentration of magnetic Mn's nearly equal to 4.5 mJ K/mol of Mn. Therefore our present value of C_N is equivalent to that due to the presence of 2000 ppm of magnetic Mn's, i.e., orders of magnitude larger than the concentration of magnetic atoms deduced from our magnetic measurements.

So, we conclude that, as in pure hexagonal Re,[41] the actual origin of C_N is due to the other possible source of hyperfine interaction which is that of the quadrupolar moments Q carried by the different nuclei with local gradients of electric field. Nuclei of Al^{27}, Re^{185}, Re^{187} and Pd^{105} carry a nuclear spin $I=5/2$ and a quadrupolar moment Q which is large for Re^{185} ($Q=2.7$ barn, 37% of natural abundance) and Re^{187} ($Q=2.6$ barn, 63% of natural abundance), and rather weak for Pd^{105} ($Q=0.8$ barn, 22% of natural abundance) and Al^{27} ($Q=0.15$ barn, 100% of natural abundance).[42] It results in a Schottky anomaly due to the splitting of nuclear energy levels and which can be expanded in powers of T^{-1} on the high-temperature side. The leading term of the nuclear specific heat is given by the expression

$$C_N T^{-2} = \sum_{i\,j} C_N^{i\,j} T^{-2},$$

$$C_N^{ij} = \alpha \frac{R}{80} \frac{(I+1)(2I+3)}{I(2I-1)} \left(\frac{e^2 q_j Q_i}{k_B} \right)^2, \qquad (5)$$

where $C_N^{ij} T^{-2}$ is the contribution of one nucleus of species i (concentration x_i) located at site j, k_B is the Boltzmann's constant, R is the gas constant. Here eq_j is the largest component at site j of the electric-field-gradient tensor in the local set of axes, known as the principal axes of the electric-field gradient (EFG). These axes are not necessarily connected to the crystallographic axes or local cluster directions. They are chosen such that the off-diagonal terms of the tensor of the local electric-field gradient equal zero. In the literature, eq is also denoted $V_{zz}=(\partial^2 V/\partial z^2)$, where V is the electric potential. In the simplest case, where the electric field is of axial symmetry, the coefficient α in Eq. (5) is equal to 1. *A priori*, it is difficult to guess the relative weight of the contribution of each element (Al, Pd, and Re) to C_N. Indeed, to point out the large magnitude of Q for Re, compared to that of Al and Pd, does not prove that Re provides the dominant contribution to C_N. First the concentration x_i

of each element in the compound is very different: for instance, $x_{Al} \approx 8 x_{Re}$. Moreover, the value of the electric-field gradient eq can be very different at Al, Pd, and Re nuclear sites, due to EFG origins possibly specific for each atomic species or for each type of local environment. It exists a way to estimate the Al and Pd contributions to C_N, based on the comparison of our present results with those obtained in closely related quasicrystals: *i*-AlPdMn and *i*-AlCuFe. Our approach is based on the isomorphism of the structures and the similarity of the chemical composition for these three *i*-phases (see Sec. II). Thus we assume that the origin and the magnitude of the EFG at the Al and Pd nuclear sites are rather similar in these three phases. This allows us to discard the possible sizeable contribution to C_P due to Al and Pd nuclei in the present case. Indeed, let us refer to specific-heat data which we obtained for *i*-AlPdMn ribbons and AlCuFe ingots, using the same experimental method and about the same time span at low *T*. In the case of *i*-AlPdMn, to avoid the magnetic hyperfine term due to magnetic Mn's, we are interested in the less magnetic *i* phase of composition i-$Al_{70.5}Pd_{22}Mn_{7.5}$, almost similar to that of our sample i-$Al_{70.5}Pd_{21}Re_{8.5}$. Then, we found a slight upturn in $C_p(T)$ below 100 mK,[36] probably due to the occurence of a magnetic ordering.[43] This upturn cannot be fitted by a T^{-2} law but the presence of a hyperfine contribution cannot be excluded with a maximum value of C_N, if it exists, of 0.2 μJ K/mol. This value is smaller than that of C_N found in *i*-AlPdRe by a factor 40. This allows us to conclude that the Al and Pd nuclei cannot contribute sizeably to C_N in AlPdRe. Concerning Al, the latter conclusion is reinforced by the comparison of the present C_p data with those previously obtained for two different ingots of i-$Al_{63}Cu_{25}Fe_{12}$,[23] then we found values of $C_N \leqslant 2 \times 10^{-2}$ μJ K/mol, which are smaller by orders of magnitude than that found for *i*-AlPdRe. Thus we conclude that the hyperfine nuclear term in *i*-AlPdRe originates almost totally in Re atoms. From Eq. (5), we find the order of magnitude of the EFG at Re site:

$$\langle (eq_{Re})^2 \rangle^{1/2} \approx 210^{15} \text{ esu/cm}^3.$$

Here $\langle (eq)^2 \rangle$ is the value of the square of the eq's for Re atoms which has to be averaged over the EFG distribution at all Re sites, due to the expected multiplicity of nonequivalent sites in quasicrystals. Now, let us discuss the magnitude of the EFG. It is large, even larger than that of pure hexagonal Re.[41] This questions the symmetry of the Re sites. Indeed, the quadrupole coupling vanishes if the nucleus is surrounded by electric charges of symmetry equal to or higher than cubic. But, we emphasize that the EFG originates in the total spatial distribution of the electric charges (both electrons and nuclei), the symmetry of which may not coincide with that of the atomic positions. Thus, to find a large EFG does not discard the possibility for Re to lie at a crystallographic site of high symmetry. It is probably the case since *i*-AlPdRe contains atoms of three different species of different valencies, i.e., of different ionic charges, which should lead to a low symmetry in terms of ionic charges even though of a high symmetry for the atomic positions. Also we note that even the first nearest neighbors of Re (Al following extended X-ray-absorption fine structure results[44]) can provide a large EFG even if they are of the same species and even if they lie at the vertices of a geometrical object of high symmetry. It is the case for instance in the structural model of Katz and Gratias, developed initially for *i*-AlCuFe,[45] and generalized for *i*-AlPd(Mn,Re).[46] The same applies for the model of Boudard *et al.*[47] built for *i*-AlPdMn. There, the Re atom is at the center of a dodecahedron which is of high symmetry. But due to steric constraints (two atoms cannot be first nearest neighbors), the probability of atomic occupancy at the vertices of the dodecahedron is not equal to 1, which results in an ionic environment which is of low symmetry.

VII. CONCLUSION

We have investigated the low-*T* specific heat of an *i*-AlPdRe sample, also characterized by magnetic susceptibility and electrical resistivity. From resistivity measurements, we believe that our system lies on the insulating side of a metal-insulator (MI) transition. We have shown that no sizeable *T*-linear term can be extracted from our specific-heat data obtained below 1 K. In contrast, the specific heat exhibits a nonlinear term T^a ($a \approx 0.1$–0.3) below 1 K, while a γT term of low value can be recovered above 1 K. This behavior is similar to that previously observed for systems lying on the insulating side of a MI transition. Concerning the hyperfine term, we showed that it is of quadrupolar origin and can be unambiguously attributed to the Re nuclei, from a comparison with specific-heat data of *i*-AlCuFe and *i*-AlPdMn. This shows the existence of large electric-field gradients at Re sites, which, nevertheless, cannot discard available structural models which involve a high symmetry of Re sites in spatial average.

ACKNOWLEDGMENTS

We are grateful to G. Fourcaudot and C. Gignoux for their precious help in preparing the samples. We warmly acknowledge R. Bellissent, D. Gratias, F. Hippert, D. Mayou, and B. Minos-Stesz for fruitful discussions.

[1] F.S. Pierce, Q. Guo, and S.J. Poon, Phys. Rev. Lett. **73**, 2220 (1994).

[2] C. Gignoux, C. Berger, G. Fourcaudot, J.C. Grieco, and H. Rakoto, Europhys. Lett. **39**, 171 (1997).

[3] J. Delahaye, J.P. Brison, and C. Berger, Phys. Rev. Lett. **81**, 4204 (1998).

[4] G. Trambly de Laissardière and D. Mayou, Phys. Rev. B **55**, 2890 (1997).

[5] C. Janot, Phys. Rev. B **53**, 181 (1996).

[6] D. Mayou, S. Roche, G. Trambly de Laissardière, C. Berger, and C. Gignoux, in *Quasicrystals*, edited by S. Takeuchi and T. Fujiwara (World Scientific, Singapore, 1998), p. 555.

[7] M.A. Chernikov, A. Bianchi, E. Felder, U. Gubler, and H.R. Ott, Europhys. Lett. **35**, 431 (1996).

[8] C. Berger, C. Gignoux, T. Wagner, T. Grenet, G. Fourcaudot, J.C. Grieco, Y. Calvayrac, and J.C. Lasjaunias, in *Rapidly*

Quenched Metastable Materials, edited by P. Duhaj, P. Mrafko, and P. Svec (Elsevier, Amsterdam, 1997), p. 406.
[9] X. Wu, S.W. Kycia, C.G. Olson, P.J. Benning, A.I. Goldman, D.W. Lynch, Phys. Rev. Lett. **75**, 4540 (1995).
[10] J. Delahaye, C. Berger, T. Grenet, T. Schaub, H. Guyot, J.P. Brison, A. Taleb-Ibrahimi, and R. Belkhou, *XXXIVth Rencontres de Moriond: Quantum Physics at Mesoscopic Scale* (Les Arcs, 1999), (Editions Frontières, in press).
[11] D. Davydov, D. Mayou, C. Berger, C. Gignoux, D. Neumann, A.G.M. Jansen, and P. Wyder, Phys. Rev. Lett. **77**, 3173 (1996).
[12] T. Schaub, J. Delahaye, C. Gignoux, C. Berger, G. Fourcaudot, F. Giroud, T. Grenet, and A.G.M. Jansen, J. Non-Cryst. Solids **250-252**, 874 (1999).
[13] R. Escudero, J.C. Lasjaunias, Y. Calvayrac, and M. Boudard, J. Phys.: Condens. Matter **11**, 383 (1999).
[14] X.-P. Tang, E.A. Hill, S.K. Wonnell, S.J. Poon, and Y. Wu, Phys. Rev. Lett. **79**, 1070 (1997).
[15] V. Simonet, F. Hippert, C. Gignoux, C. Berger, and Y. Calvayrac, in *Quasicrystals* (Ref. 6), p. 696.
[16] M. Rodmar, D. Oberschmidt, M. Ahlgren, C. Gignoux, J. Delahaye, C. Berger, S.J. Poon, and Ö. Rapp, J. Non-Cryst. Solids **250-252**, 883 (1999).
[17] M. Rodmar, M. Ahlgren, D. Oberschmidt, C. Gignoux, J. Delaye, C. Berger, S.J. Poon, and Ö. Rapp, Phys. Rev. B (to be published).
[18] J. Delahaye and C. Berger (unpublished).
[19] M. Boudard, M. de Boissieu, C. Janot, J.M. Dubois, and C. Dong, Philos. Mag. Lett. **64**, 197 (1991).
[20] Q. Guo and S.J. Poon, Phys. Rev. B **54**, 12 793 (1996).
[21] F.S. Pierce, S.J. Poon, and Q. Guo, Science **261**, 737 (1993).
[22] F. Zougmoré, J.C. Lasjaunias, and O. Béthoux, J. Phys. (France) **50**, 1241 (1989).
[23] J.C. Lasjaunias, Y. Calvayrac, and Hongshun Yang, J. Phys. I **7**, 959 (1997).
[24] J.J. Préjean, J.C. Lasjaunias, and C. Berger (unpublished).
[25] N. Vernier, G. Bellessa, B. Perrin, A. Zarembowitch, and M. de Boissieu, Europhys. Lett. **22**, 187 (1993).
[26] M.A. Chernikov, A.D. Bianchi, and H.R. Ott, Phys. Rev. B **51**, 153 (1995).
[27] J. Dolinšek, B. Ambrosini, P. Vonlanthen, J.L. Gavilano, M.A. Chernikov, and H.R. Ott, Phys. Rev. Lett. **81**, 3671 (1998).
[28] A. Ravex, J.C. Lasjaunias, and O. Bethoux, Physica B & C **B107**, 395 (1981); Solid State Commun. **40**, 853 (1981).
[29] M.A. Paalanen, J.E. Graener, and R.N. Bhatt, Phys. Rev. Lett. **61**, 597 (1988); see also M. Lackner and H.v. Löhneysen, *ibid.* **63**, 648 (1989); H. Kamimura, in *Electron-Electron Interactions in Disordered Systems*, edited by A.L. Efros and M. Pollack (North-Holland, Amsterdam, 1985).
[30] S. Hunklinger and A.K. Raychaudhuri in *Progress in Low Temperature Physics*, edited by D.F. Brewer (Elsevier, New York, 1986), Vol. IX, Chap. 3.
[31] C. Berger, D. Mayou, and F. Cyrot-Lackman, in *Quasicrystals*, edited by C. Janot and R. Mosseri (World Scientific, Singapore, 1995), p. 423.
[32] U. Mizutami, J. Phys.: Condens. Matter **10**, 4609 (1998).
[33] Ö. Rapp, in *Physical Properties of Quasicrystals*, edited by Z.M. Stadnik, Springer Series in Solid State Physics Vol. 126 (Springer, Berlin, 1998).
[34] A.D. Bianchi, F. Bommeli, M.A. Chernikov, U. Gubler, L. Degiorgi, and H.R. Ott, Phys. Rev. B **55**, 5730 (1997).
[35] M.A. Chernikov (private communication).
[36] J.C. Lasjaunias (unpublished).
[37] J.C. Lasjaunias, J.L. Tholence, C. Berger, and D. Pavuna, Solid State Commun. **64**, 425 (1987).
[38] J.J. Préjean, J.C. Lasjaunias, A. Sulpice, D. Mayou, and C. Berger, in *Quasicrystals* (Ref. 31), p. 510.
[39] K. Wang and P. Garoche, Phys. Rev. B **55**, 250 (1997).
[40] J.C. Lasjaunias, A. Sulpice, N. Keller, J.J. Préjean, and M. de Boissieu, Phys. Rev. B **52**, 886 (1995).
[41] P.E. Gregers-Hansen, M. Krusius, and G.R. Pickett, Phys. Rev. Lett. **27**, 38 (1971).
[42] *Progress in Materials Science*, edited by C.C. Carter, L.H. Bennet, and D.J. Kahan (Pergamon Press, Oxford, 1977), Vol. 20.
[43] For this sample, we expect a spin-glass transition temperature T_G of nearly 30 mK and thus a standard magnetic term in C_p appearing at $2.5T_G$. Here, T_G is estimated from the concentration of magnetic Mn's (4×10^{-4} of the total number of Mn atoms) deduced from magnetization measurements; see Ref. 38.
[44] A. Sadoc, J.S. Poon, and M. Boudard, in *Quasicrystals* (Ref. 31), p. 156.
[45] A. Katz and D. Gratias, in *Quasicrystals* (Ref. 31), p. 164.
[46] D. Gratias, in *Current Topics in Quasicrystals*, edited by E. Belin, C. Berger, M. Quiquandon, and A. Sadoc (World Scientific, Singapore, in press).
[47] M. Boudard, M. de Boissieu, C. Janot, G. Heger, C. Beeli, H-U. Nissen, H. Vincent, R. Ibberson, M. Audier, and J.M. Dubois, J. Phys.: Condens. Matter **4**, 10 149 (1992); M. Boudard (private communication).